A Low-Complexity Detection Algorithm for Generalized Space Shift Keying Systems

Xinhe Zhang, Haoran Tan, and Wenbo Lv

Abstract—**Generalized space shift keying (GSSK) transmits signals through antenna indices, which can overcome the problems of inter-channel interference (ICI), inter-antenna synchronization (IAS) and multiple radio frequency (RF) chains in traditional MIMO technology, and provide a new method for the application of next-generation large-scale MIMO technology. However, maximum likelihood (ML) detection has high complexity, which greatly increases the detection time. A new detection algorithm, termed as PS-ML algorithm, which combines the idea of probability sorting (PS) and ML detection, is proposed in this paper. Simulation results show that the proposed detector makes a good tradeoff between the BER performance and the complexity.**

Index Terms—**Generalized space shift keying (GSSK), spatial modulation (SM), probability sorting, maximum likelihood(ML), multiple input multiple output (MIMO).**

I. Introduction

SPATIAL modulation (SM) is a promising multiple input multiple output (MIMO) scheme, which encodes information in the combination of antenna indices and the conventional phase and amplitude [1]-[4]. Only one transmit antenna is activated in each time slot, which effectively avoids inter-channel interference (ICI). The SM systems simultaneously utilize the signal constellation and the space constellation to convey information. Compared to MIMO systems, SM systems have a lower spectral efficiency. In order to further increase spectral efficiency, the generalized SM (GSM) was proposed to activate multiple transmit antennas [5]-[6]. In SM and GSM systems, the detector needed to jointly detect the activated antenna indices and the transmitted symbols at the receiver. Thus, the common drawback of SM and GSM is the higher detection complexity. As a simplified variant of SM, space shift keying (SSK) only utilizes antenna indices to carry information [7]-[9], which can greatly decrease the complexity. Compared with SM and SSK, SSK has a less-complicated detection process at the receiver. By allowing multiple transmitting antennas to be activated, the generalized SSK (GSSK) modulation improves the transmission rate[10]-[12].

For GSSK, the optimal maximum likelihood (ML) detector [10] searches all possible transmit antenna combinations (TACs), the complexity grows exponentially in the number of TACs. Especially, the computational complexity is prohibitive in large-scale MIMO systems. Recently, various low-complexity optimal or sub-optimal detectors for GSSK systems have been proposed. In [13], Liu *et al.* proposed a novel detection algorithm for massive GSSK systems, which is based on the penalty function and likelihood ascent search. In [14], Chang et al. proposed greedy column search (GCS), convex superset relaxation (CSR), and semidefinite relaxation (SDR) detectors, but the detectors show poor bit error ratio (BER) performance. When the transmitted signal has the sparse characteristic, the compressive sensing (CS) can be used to the detection of GSSK [15]-[19], and GSM [20]-[22]. The normalized CS (NCS) algorithm proposed in [15], has a lower computational complexity than that of ML detector. Since the NCS detector is based on the orthogonal matching pursuit (OMP) algorithm [23], which is an iterative algorithm and suffers from the error propagation. To further improve the performance of NCS detector, two OMP-based detectors were developed in [16]. In the two detectors, two matrices are designed to satisfy that the equivalent channel gain matrix is approximately orthogonal. The performance can be further improved, but the error propagation phenomenon still exists. In [18], Peng *et al.* proposed a sparse K-best (SK) detector based on the conventional K-best detector applied in MIMO systems by exploiting the sparse property of GSSK signal. In [17], Kallummil *et al.* proposed a detector based CS and ML. The detector involved a superset selection using CS algorithm which is followed by the ML search. The CS-based detectors aforementioned can reduce the performance gap with ML detector.

A novel detector based on probability sorting and ML strategies, termed as PS-ML detector, is developed in this paper. The main contributions of this paper are summarized as follows:

- First of all, a probability sorting strategy is used to estimate the TACs. The TACs is estimated in descending order of probability value.
- Secondly, the preset threshold value is used to decrease the computational complexity. If the Euclidean distance of the estimated signal is within the threshold value, then the estimated signal is considered as the result. The preset threshold value can balance the tradeoff between the complexity and the BER performance.
- Thirdly, the effect of the preset threshold value on the proposed algorithm is demonstrated by simulations.
- Finally, we compare the complexity and the BER performance of the proposed detector with NCS detector and ML detector.

The rest of this paper is organized as follows. Section II gives the system model of GSSK systems. The detectors for

Manuscript received October 4, 2021; revised February 9, 2022. This work was supported in part by the Doctoral Scientific Research Foundation of Liaoning Province (Grant No. 2020-BS-225) and the Scientific Research Fund of Liaoning Provincial Education Department of China (Grant No. LJKZ0292).

Xinhe Zhang is an Associate Professor of School of Electronic and Information Engineering, University of Science and Technology Liaoning, Anshan, 114051 China. (corresponding author, phone: 86-412-5929738; email: 527075114@qq.com).

Haoran Tan is a Postgraduate of School of Electronic and Information Engineering, University of Science and Technology Liaoning, Anshan, 114051 China. (email: 853386218@qq.com).

Wenbo Lv is a Postgraduate of School of Electronic and Information Engineering, University of Science and Technology Liaoning, Anshan, 114051 China. (email: 1273795029@qq.com).

GSSK are given in Section III. The proposed detector is presented in Section IV. The BER performance and complexity of different detectors are analyzed in Section V. Section VI concludes the paper.

Notation: Upper and lower case boldface letters denote matrices and column vectors, respectively. $(\cdot)^T$, $(\cdot)^H$, and $(\cdot)^{-1}$ represent transpose, Hermitian transpose, and inversion operations, respectively. $\|\cdot\|_p$ denotes the ℓ_p norm of a vector, $\lfloor\cdot\rfloor$ denotes the floor operation, $|\cdot|$ stands for the absolute value of a complex number or the cardinality of a given set, ϕ stands for the empty set. $\Re(\cdot)$ and $\Im(\cdot)$ represent the real and imaginary parts of a variable, respectively. $\binom{n}{k}$ denotes the binomial coefficient, which is given by $\binom{n}{k} = \frac{n!}{k!(n-k)!}$. If $n < k$, $\binom{n}{k}$ is defined to be zero. The relative complement of $\mathcal{A}$ in $\mathcal{B}$ is denoted by $\mathcal{B}\backslash\mathcal{A}$. $\mathcal{CN}\left(\mu, \sigma^2\right)$ denotes the complex normal distribution of a random variable with a mean μ and variance σ^2. $\mathbb{R}^{m\times n}$ and $\mathbb{C}^{m\times n}$ represent the set of real-valued, complex-valued matrices with m rows and n columns, respectively.

II. System Model

Consider a multi-antenna system with N_T transmit antennas and N_R receive antennas. In GSSK systems, N_P out of N_T transmit antennas are activated for data transmission, therefore $N_C' = \binom{N_T}{N_P}$ legitimate transmit antenna combinations are available. However, the number of possible TACs in the spatial constellation diagram is generally a power of 2. Hence, in GSSK systems, we select $N_C = 2^{\left\lfloor \log_2 \binom{N_T}{N_P} \right\rfloor}$ TACs out of N_C' combinations for antenna selection, where $\lfloor\cdot\rfloor$ denotes the floor operation. The incoming binary source is divided into blocks of N_C bits. The N_C bits block is used to select a TAC $\mathcal{A}_i$, $i \in (1, \cdots, N_C)$.

Assuming with quasi-static flat Rayleigh fading channels, the received signal vector $\mathbf{y} \in \mathbb{C}^{N_R\times 1}$ can be formulated as

$$\mathbf{y} = \mathbf{H}\cdot\mathbf{x} + \mathbf{n}, \tag{1}$$

where $\mathbf{x} \in \mathbb{R}^{N_T\times 1}$ represents the transmitted signal vector. Since N_P antennas are activated at each time slot, there are N_P '1's in $\mathbf{x}$ leaving the rest of elements in $\mathbf{x}$ '0's. $\mathbf{H} \in \mathbb{C}^{N_R\times N_T}$ denotes the channel gain matrix, whose entries follow identically independent distributed (i.i.d.) circular symmetric complex Gaussian distribution $\mathcal{CN}(0, 1)$. $\mathbf{n} \in \mathbb{C}^{N_R\times 1}$ is the additive white Gaussian noise (AWGN) vector, whose entries from $\mathcal{CN}\left(0, \sigma^2\right)$. The transmitted signal vector $\mathbf{x}$ is drawn equally probably from the constellation set $\mathcal{X} = \left\{[x_1, x_2, \cdots, x_{N_T}] \middle| \sum_{j=1}^{N_T} x_j = N_P, x_j \in \{0, 1\}\right\}$ with $|\mathcal{X}| = N_C$. The transmitted signal vector $\mathbf{x}$ can be expressed as

$$\mathbf{x} = \left[\cdots, 0, \underbrace{1}_{j_1}, 0, \cdots, 0, \underbrace{1}_{j_2}, 0, \cdots 0, \underbrace{1}_{j_{N_P}}, 0, \cdots\right]^T, \tag{2}$$

where $(j_1, \cdots, j_{N_P})$ denotes the activated TA indices.

Especially, the received signal vector given by Eq. (1) can also be formulated as

$$\mathbf{y} = \sum\nolimits_{t=j_1}^{j_{N_P}} \mathbf{h}_t + \mathbf{n}, \tag{3}$$

where $\mathbf{h}_t$ is the t-th column of channel gain matrix $\mathbf{H}$.

III. GSSK Detectors

In this section, a brief overview of the detectors for GSSK systems is given.

A. ML Detector

The ML detector has the optimal performance BER by exhaustively searching through all TACs as

$$\hat{\mathbf{x}}_{ML} = \arg\min_{\mathbf{x}\in\mathcal{X}} \|\mathbf{y} - \mathbf{H}\cdot\mathbf{x}\|_2^2. \tag{4}$$

In fact, the receiver aims to detect the activated transmit antenna indices. The simplified ML detector can be expressed as

$$\hat{J} = \arg\min_{j\in\mathcal{A}_i, i\in\{1,\cdots,N_C\}} \left\|\mathbf{y} - \sum\nolimits_{t=j_1}^{j_{N_P}} \mathbf{h}_t\right\|_2^2. \tag{5}$$

B. NCS Detector

In [15], an OMP-based NCS detector was proposed. The Eq. (1) is rewritten in real-valued form as

$$\bar{\mathbf{y}} = \underbrace{\begin{bmatrix} \Re(\mathbf{y}) \\ \Im(\mathbf{y}) \end{bmatrix}}_{\bar{\mathbf{y}}} = \underbrace{\begin{bmatrix} \Re(\mathbf{H}) \\ \Im(\mathbf{H}) \end{bmatrix}}_{\bar{\mathbf{H}}} \cdot \mathbf{x} + \underbrace{\begin{bmatrix} \Re(\mathbf{n}) \\ \Im(\mathbf{n}) \end{bmatrix}}_{\bar{\mathbf{n}}} = \bar{\mathbf{H}}\cdot\mathbf{x} + \bar{\mathbf{n}}, \tag{6}$$

where $\Re(\cdot)$ and $\Im(\cdot)$ denote the real and imaginary components of a complex-valued number, respectively. After real-valued transformation, $\bar{\mathbf{y}} \in \mathbb{R}^{2N_R\times 1}$, $\bar{\mathbf{H}} \in \mathbb{R}^{2N_R\times N_T}$, and $\bar{\mathbf{n}} \in \mathbb{R}^{2N_R\times 1}$. After normalizing each column of $\mathbf{H}$, the signal can be recovered by the NCS algorithm, which is shown in Table I.

TABLE I
PSEUDO CODE OF NCS DETECTOR

Input: $\mathbf{y}$, $\mathbf{H}$, N_P, $\mathbf{r}_0 = \mathbf{y}$, $\Lambda = \phi$.
Output: $\hat{J}$.
for $j = 1$ to N_T **do**
  $\tilde{\mathbf{h}}_j = \frac{\mathbf{h}_j}{\|\mathbf{h}_j\|_2}$;
end for
$\bar{\mathbf{y}} = \underbrace{\begin{bmatrix} \Re(\mathbf{y}) \\ \Im(\mathbf{y}) \end{bmatrix}}_{\bar{\mathbf{y}}} = \underbrace{\begin{bmatrix} \Re(\tilde{\mathbf{H}}) \\ \Im(\tilde{\mathbf{H}}) \end{bmatrix}}_{\bar{\mathbf{H}}} \cdot \mathbf{x} + \underbrace{\begin{bmatrix} \Re(\mathbf{n}) \\ \Im(\mathbf{n}) \end{bmatrix}}_{\bar{\mathbf{n}}} = \bar{\mathbf{H}}\cdot\mathbf{x} + \bar{\mathbf{n}}.$
for $t = 1$ to N_P **do**
  $\lambda = \max\left(|\bar{\mathbf{H}}^T\mathbf{r}_{t-1}|\right)$;
  $\Lambda_t = \Lambda_{t-1} \cup \lambda_t$;
  $\mathbf{x}_t = \arg\min_{\mathbf{x}} \|\bar{\mathbf{y}} - \bar{\mathbf{H}}_{\Lambda_t}\mathbf{x}\|_2^2 = \left(\bar{\mathbf{H}}_{\Lambda_t}^T\bar{\mathbf{H}}_{\Lambda_t}\right)^{-1}\bar{\mathbf{H}}_{\Lambda_t}^T\bar{\mathbf{y}}$;
  $\mathbf{r}_t = \bar{\mathbf{y}} - \bar{\mathbf{H}}_{\Lambda_t}\mathbf{x}_t$;
end for
$\hat{J} = \Lambda$.

IV. The Proposed Detector

At the receiver, the demodulator firstly identifies the activated antenna indices based on the received signal and channel gain matrix, and then obtains the transmitted symbols based on the GSSK mapping rule.

The NCS detector developed in [15], which is based on the OMP detector, has a significant lower computational complexity than that of the ML detector. However, since the OMP-based detector suffers from error propagation, the BER performance of NCS detector is much worse than ML detector.

In this section, we propose a new low complexity detector, termed as probability sorting ML (PS-ML) detector. The proposed PS-ML detector works as follows.

First of all, the real-valued system model is shown in Eq. (6). In the proposed algorithm, an ordering strategy is firstly adopted to sort all transmit antennas. That is, we calculate the inner product of each column of real-valued channel gain matrix $\bar{\mathbf{H}}$ and the received signal $\bar{\mathbf{y}}$ to obtain the new sequence as

$$\mathbf{p} = [p_1, p_2, \cdots, p_k, \cdots, p_{N_T}] = \arg sort(|\bar{\mathbf{H}}^T \bar{\mathbf{y}}|), \quad (7)$$

where $sort(\cdot)$ denotes the descending order function; p_1 and p_{N_T} denote the indices of the maximum and minimum elements of $|\bar{\mathbf{H}}^T \bar{\mathbf{y}}|$, respectively.

Next, we obtain the new TACs search order by searching the TACS in ascending order of $\mathbf{p}$. The new search order Θ can be obtained by

$$\Theta \leftarrow \Theta \cup (row\_index \backslash \Theta), \quad (8)$$

$$row\_index = search(p_k, \mathcal{A}), \quad (9)$$

where function $search(\cdot)$ returns the row indices including p_k from the set $\mathcal{A}$.

The preset threshold $V_{th} = \beta N_R \sigma^2$ is employed to judge whether the TAC is reliable or not. We determine whether or not the Euclidean distance (ED) of the estimated transmit antenna indices is inside the threshold V_{th}. If the ED satisfies

$$\left\| \bar{\mathbf{y}} - \sum\nolimits_{j=1}^{N_p} \bar{\mathbf{h}}_{\mathcal{A}(\Theta(i),j)} \right\|_2^2 < V_{th}, \quad (10)$$

then the output $\mathcal{A}(\Theta(i), :)$ is considered as the final detection result. If no output satisfied the above, the final result is taken as

$$\hat{J} = arg \min_{\Theta} \left\| \bar{\mathbf{y}} - \sum\nolimits_{j=1}^{N_p} \bar{\mathbf{h}}_{\mathcal{A}(\Theta(i),j)} \right\|_2^2. \quad (11)$$

The detection processes of the proposed PS-ML detector are summarized in Table II.

TABLE II
PSEUDO CODE OF PS-ML DETECTOR

Input: $\mathbf{y}$, $\mathbf{H}$, N_P, $\Theta = \phi$, $\mathcal{A}$, and the size of set $\mathcal{A}$ is N_C.
Output: $\hat{J}$.
Reshape the system model by $\bar{\mathbf{y}} = \bar{\mathbf{H}} \cdot \mathbf{x} + \bar{\mathbf{n}}$;
$\mathbf{p} = [p_1, p_2, \cdots, p_k, \cdots, p_{N_T}] = \arg sort(|\bar{\mathbf{H}}^T \bar{\mathbf{y}}|)$;
for $k = 1$ to N_T **do**
  $row\_index = search(p_k, \mathcal{A})$, where function $search(\cdot)$ returns the row indices including p_k from the set $\mathcal{A}$;
  $\Theta \leftarrow \Theta \cup (row\_index \backslash \Theta)$;
end for
for $i = 1$ to N_C **do**
  $\delta(i) = \left\| \bar{y} - \sum_{j=1}^{N_P} \bar{\mathbf{h}}_{\mathcal{A}(\Theta(i),j)} \right\|_2^2$;
  if $\delta(i) < V_{th}$ **then**
    $\hat{J} = \mathcal{A}(\Theta(i), :)\,; return$;
  end if
end for
$idx = \arg\min(\delta)$;
$\hat{J} = \mathcal{A}(\Theta(idx), :)$.

V. Simulation Results

In order to verify the effectiveness of the proposed PS-ML detector, a series of simulation experiments have been done on platform with i5-10210U processor and 16G memory. In this section, the comparison of the BER performance and complexity among ML detector, NCS detector and the proposed PS-ML detector are presented. The BER performance and complexity are simulated under the assumption of ideal channel state information at receiver.

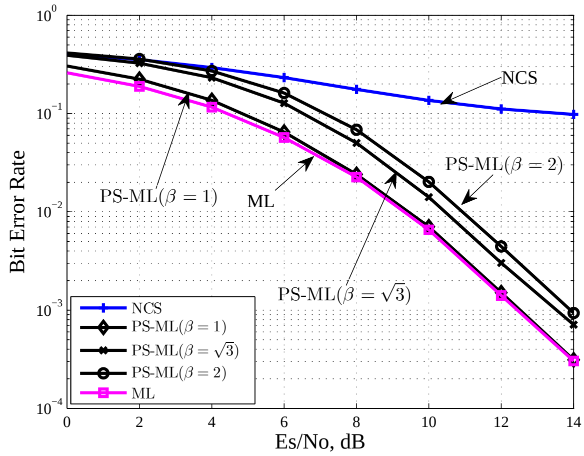

Fig. 1. BER performance comparison of above-mentioned detectors for GSSK systems with $N_T = 10$, $N_R = 4$ and $N_P = 2$.

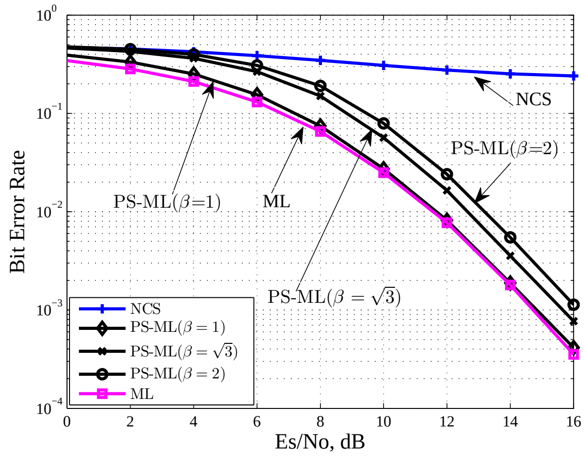

Fig. 2. BER performance comparison of above-mentioned detectors for GSSK systems with $N_T = 10$, $N_R = 4$ and $N_P = 3$.

A. BER Performance Comparison

We assume that the channel is a quasi-static flat Rayleigh fading channel, additive white Gaussian noise obeys the distribution with the mean value of 0 and variance of 1. With the increase of the number of active antennas, the spectral efficiency and hardware cost of the GSSK systems will increase significantly. Therefore, we consider a GSSK system with $N_p \ll N_T$. Since it is difficult to employ a large number of antennas at the receiver side of the downlink, and hence we assume $N_R < N_T$.

The BER performance curves of all above-mentioned detectors under two different GSSK systems are simulated. The parameters are set as follows: 1) $N_T = 10$, $N_R = 4$, $N_P = 2$; and 2) $N_T = 10$, $N_R = 4$, $N_P = 3$. The simulation results are shown in Figs. 1 and 2.

It can be seen from Figs. 1 and 2 that the BER performance of PS-ML detector under different thresholds is obviously better than that of NCS detector. The main reason is as follows: the higher the transmit antenna ranking in Eq. (7), the more likely it is the optimal solution. The preset threshold reduces the average search times. Meanwhile, we notice that the larger the threshold is, the worse the BER performance of the proposed PS-ML algorithm is. When the preset threshold decreases to a certain value, the BER performance of the proposed PS-ML algorithm will be equivalent to that of ML algorithm.

B. Complexity analysis

ML Detector:

The conventional ML detection algorithm is equivalent to searching all the TACs. It can be expressed as

$$\hat{J} = \arg \min_{j \in \mathcal{A}_i, i \in \{1,\cdots,N_C\}} \left\| \mathbf{y} - \sum\nolimits_{t=j_1}^{j_{N_P}} \mathbf{h}_t \right\|_2^2. \quad (12)$$

According to Eq. (12), $\sum_{t=j_1}^{j_{N_P}} \mathbf{h}_t$ requires $2N_R N_P$ real-valued flops, $\mathbf{y} - (\cdot)$ requires $2N_R$ real-valued flops, $\|\cdot\|_2^2$ requires $4N_R - 1$ real-valued flops. In each search, the operation $\left\| \mathbf{y} - \sum_{t=j_1}^{j_{N_P}} \mathbf{h}_t \right\|_2^2$ requires $2N_R N_P + 6N_R - 1$ real-valued flops. The operation is repeated N_C times, thus the complexity of the conventional ML detector is about $(2N_R N_P + 6N_R - 1)N_C$, where N_C represents the number of TACs.

NCS Detector:

In NCS detector (shown in Table I), lines 2, 6, 8, and 9 require $6N_R - 1$, $4N_T N_R$, $4t^3 + (8N_R + 7)t^2 + (2N_R - 1)t$, $4N_R t$ real-valued flops, respectively. Where $t \in \{1, \cdots, N_P\}$. The operation in line 2 is computed N_T times and those in lines 6, 8, and 9 are computed N_P times. Therefore, the complexity of NCS detector is about $N_T (6N_R - 1) + 4N_T N_R N_P + \sum_{t=1}^{N_P} 4t^3 + (8N_R + 7) t^2 + (6N_R - 1) t$.

The Proposed PS-ML Detector:

In PS-ML detector (shown in Table II), the complexity is dominated by lines 2 and 8. Lines 2 and 8 require $4N_T N_R$, $2N_R N_P + 6N_R - 1$ real-valued flops, respectively. The operation in line 2 is calculated only one time, however those in line 8 is calculated k times, where $1 \le k \le N_C$. k varies in each running of the algorithm. The average complexity can only be obtained through simulation. The average complexity of PS-ML detector is about $4N_T N_R + (2N_R N_P + 6N_R - 1)\bar{k}$, where $\bar{k}$ denotes the average times of operations performed in lines 7-12.

Figs. 3 and 4 illustrate the average complexity of the above-mentioned detectors for GSSK systems with $N_T = 10$, $N_R = 4$, $N_P = 2$ and $N_T = 10$, $N_R = 4$, $N_P = 3$, respectively. One can observe from Figs. 3 and 4 that the proposed PS-ML detectors with $V_{th} = N_R \sigma^2$, $V_{th} = \sqrt{3} N_R \sigma^2$, $V_{th} = 2N_R \sigma^2$ are capable of achieving about 20%, 60%, 64% reduction in complexity over ML detector, respectively. The higher the threshold is, the lower the complexity of the algorithm is. The complexity of PS-ML detector varies with the threshold. When the threshold is small, the complexity of PS-ML detector is larger than OMP detector. If the threshold is large, the complexity of PS-ML detector is lower than OMP detector.

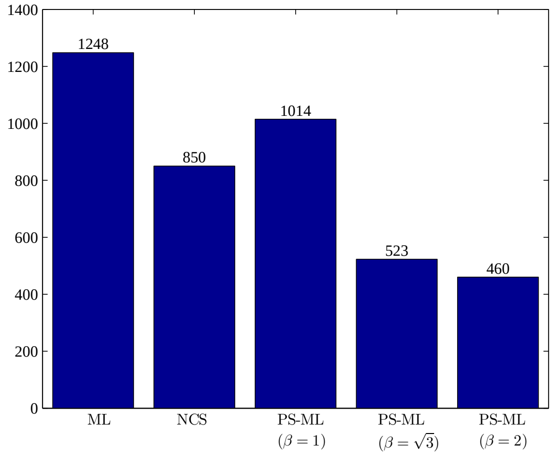

Fig. 3. Complexity comparison of above-mentioned detectors for GSSK systems with $N_T = 10$, $N_R = 4$ and $N_P = 2$.

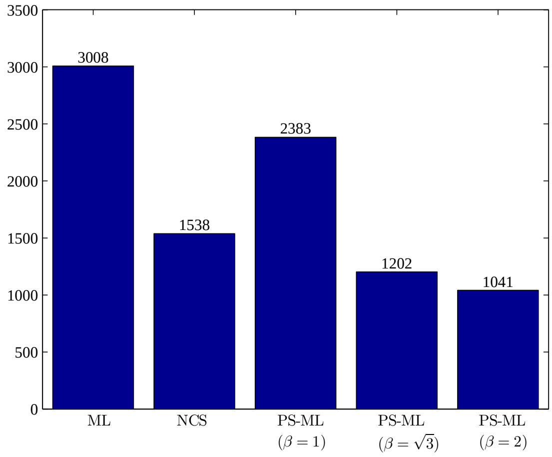

Fig. 4. Complexity comparison of above-mentioned detectors for GSSK systems with $N_T = 10$, $N_R = 4$ and $N_P = 3$.

In conclusion, the probability sorting strategy and the preset threshold have an effect on the BER performance and complexity of PS-ML algorithm. The smaller the threshold is, the higher the complexity is. The proposed PS-ML detector can obtain a flexible trade-off between the BER performance and the complexity.

VI. Conclusion

GSSK technology provides a new method and idea for the research and application of next generation large-scale MIMO communication, which is of great significance. In this paper, the PS-ML detector, which combines the idea of probability sorting and ML detection, is proposed for GSSK systems. Simulation results show that the probability sorting strategy and the preset threshold make a tradeoff between the BER performance and the complexity.

References

[1] R. Y. Mesleh, H. Haas, D. Sinanovic, W. A. Chang, and S. Yun, “Spatial modulation,” *IEEE Transactions on Vehicular Technology*, vol. 57, no. 4, pp. 2228-2241, Apr. 2008.

[2] R. Rajashekar, K. V. S. Hari, and L. Hanzo, "Reduced-complexity ML detection and capacity-optimized training for spatial modulation systems," *IEEE Transactions on Communications*, vol. 62, no. 1, pp. 112-125, Jan. 2014.

[3] J. Jeganathan, A. Ghrayeb, and L. Szczecinski, "Spatial modulation: Optimal detection and performance analysis," *IEEE Communications Letters*, vol. 12, no. 8, pp. 545-547, Aug. 2008.

[4] M. D. Renzo, H. Haas, and P. M. Grant, "Spatial modulation for multiple-antenna wireless systems: A survey," *IEEE Communications Magazine*, vol. 49, no. 12, pp. 182-191, Dec. 2012.

[5] M. D. Renzo, H. Haas, A. Ghrayeb, S Sugiura, and L. Hanzo, "Spatial modulation for generalized MIMO: Challenges, opportunities, and implementation," *Proceedings of the IEEE*, vol. 102, no. 1, pp. 56-103, Jan. 2014.

[6] P. Yang, M. D. Renzo, Y. Xiao, and S. Li, "Design guideline for spatial modulation," *IEEE Communications Surveys & Tutorials*, vol. 17, no. 1, pp. 6-26, Jan. 2014.

[7] J. Jeganathan, A.Ghrayeb, L. Szczecinski, and A. Ceron, "Space shift keying modulation for MIMO channels," *IEEE Transactions on Wireless Communications*, vol. 8, no. 7, pp. 3692-3703, Jun. 2009.

[8] M. D. Renzo, and H. Haas, "Improving the performance of space shift keying (SSK) modulation via opportunistic power allocation," *IEEE Communications Letters*, vol. 14, no. 6, pp. 500-502, Jun. 2010.

[9] M. D. Renzo, and H. Haas, "A general framework for performance analysis of space shift keying (SSK) modulation for MISO correlated Nakagami-m fading channels," *IEEE Transactions on Communications*, vol. 58, no. 9, pp. 2590-2603, Sep. 2010.

[10] J. Jeganathan, A. Ghrayeb, and L. Szczecinski, "Generalized space shift keying modulation for MIMO channels," IEEE 19th International Symposium on Personal, Indoor and Mobile Radio Communications, 15-18 September, 2008, Cannes, pp. 1-5.

[11] K. Ntontin, M. D. Renzo, A. Perez-Neira, and C. Verikoukis, "Adaptive generalized space shift keying," *EURASIP Journal on Wireless Communications and Networking*, vol. 1, no. 1, pp. 1-15, Jan. 2013.

[12] K. Ntontin, M. D. Renzo, A. Perez-Neira, and C. Verikoukis, "Adaptive generalized space shift keying (GSSK) modulation for MISO channels: a new method for high diversity and coding gains", 2012 IEEE Vehicular Technology Conference (VTC Fall), 3-6 September, 2012, Quebec City, pp. 1-5.

[13] W. Liu, Z. Gu, and M. Jin, "Penalty function based detector for generalized space shift keying massive MIMO systems," *IEEE Communications Letters*, vol. 20, no. 4, pp. 664-667, Apr. 2016.

[14] R. Y. Chang, W. H. Chung, and S. J. Lin, "Detection of space shift keying signal in large MIMO systems," 2012 8th International Wireless Communications and Mobile Computing Conference, 27-31 August, 2012, Limassol, pp. 1185-1190.

[15] C. M. Yu, S. H. Hsieh, H. W. Liang, C. S. Lu, W. H. Chung, S. Y. Kuo, and S. C. Pei, "Compressed sensing detector design for space shift keying in MIMO systems," *IEEE Communications Letters*, vol. 16, no. 10, pp. 1556-1559, Oct. 2012.

[16] C. M. Yu, W. H. Chung, and H. W. Liang, "OMP-based detectors design for space shift keying in large MIMO systems," 2014 IEEE Global Communications Conference, 8-12, December, 2014, Austin, pp. 4072-4076.

[17] S. Kallummil and S. Kalyani, "Combining ML and compressive sensing: detection schemes for generalized space shift keying," *IEEE Wireless Communications Letters*, vol. 5, no. 1, pp. 72-75, Jan. 2015.

[18] X. Peng, W. Wu, J. Sun, and Y. Liu, "Sparse K-best detectors for generalized space shift keying in large-scale multiple-input-multiple-output systems," *IET Communications*, vol. 9, no. 6, pp. 771-778, Jun. 2015.

[19] X. Zhang, Q. Liu, and M. Jin, "Detection of generalized space shift keying signal with sparse reconstruction," *IEEE Transactions on Vehicular Technology*, vol. 66, no. 6, pp. 5473-5477, Jun. 2017.

[20] L. Xiao, P. Yang, Y. Xiao, S. Fan, M. D. Renzo, W. Xiang, and S. Li, "Efficient compressive sensing detectors for generalized spatial modulation systems," *IEEE Transactions on Vehicular Technology*, vol. 66, no. 6, pp. 1284-1298, Jun. 2017.

[21] W. Liu, N. Wang, M. Jin, and H. Xu, "Denoising detection for the generalized spatial modulation system using sparse property," *IEEE Communications Letters*, vol. 18, no. 1, pp. 22-25, Jan. 2014.

[22] E. Candes, J. Romberg, and T. Tao, "Robust uncertainty principle: exact signal reconstruction form highly incomplete frequency information," *IEEE Transactions on Information Theory*, vol. 52, no. 1, pp. 489-509, Feb. 2006.

[23] J. A. Tropp and A. C. Gilbert, "Signal recovery from random measurements via orthogonal matching pursuit," *IEEE Transactions on Information Theory*, vol. 53, no. 12, pp. 4655-4666, Dec. 2007.

Xinhe Zhang was born in Hebei Province, P. R. China, received the B.S. degree in Application of Electronic Technology from Anshan Iron and Steel Technology, Anshan, P. R. China, the M.S. degree in Control Theory and Control Engineering from Anshan University of Science and Technology, Anshan, P. R. China, the Ph.D. degree in Communication and Information Systems from Dalian University of Technology, Dalian, P. R. China, in 2002, 2005, 2017. His research interests include signal processing and compressed sensing.

Haoran Tan received the B. S. degree in Communication Engineering from Liaoning Institute of Science and Technology, Benxi, P. R. China in 2019. She is pursuing the M. S. degree at University of Science and Technology Liaoning, Anshan, P. R. China. Her research interests include signal processing and wireless communication.

Wenbo Lv received the B. S. degree in Communication Engineering from Tongda College of Nanjing University of Posts and Telecommunications, Yangzhou, P. R. China in 2020. He is pursuing the M. S. degree at University of Science and Technology Liaoning, Anshan, P. R. China. His main research interest is signal detection.